Title
Fluorescence lifetime imaging by asynchronous pump-probe microscopy

Permalink
https://escholarship.org/uc/item/0z63d3tp

Journal
Biophysical Journal, 69(6)

ISSN
0006-3495

Authors
Dong, CY
So, PT
French, T
et al.

Publication Date
1995-12-01

DOI
10.1016/s0006-3495(95)80148-7

Peer reviewed

Fluorescence Lifetime Imaging by Asynchronous Pump-Probe Microscopy

C. Y. Dong, P. T. C. So, T. French, and E. Gratton

Laboratory for Fluorescence Dynamics, Department of Physics, University of Illinois at Urbana-Champaign, Urbana, Illinois 61801 USA

ABSTRACT We report the development of a scanning lifetime fluorescence microscope using the asynchronous, pump-probe (stimulated emission) approach. There are two significant advantages of this technique. First, the cross-correlation signal produced by overlapping the pump and probe lasers results in i) an axial sectioning effect similar to that in confocal and two-photon excitation microscopy, and ii) improved spatial resolution compared to conventional one-photon fluorescence microscopy. Second, the low-frequency, cross-correlation signal generated allows lifetime-resolved imaging without using fast photodetectors. The data presented here include 1) determination of laser sources' threshold powers for linearity in the pump-probe signal; 2) characterization of the pump-probe intensity profile using 0.28 μm fluorescent latex spheres; 3) high frequency (up to 6.7 GHz) lifetime measurement of rhodamine B in water; and 4) lifetime-resolved images of fluorescent latex spheres, human erythrocytes and a mouse fibroblast cell stained by rhodamine DHPE, and a mouse fibroblast labeled with ethidium bromide and rhodamine DHPE.

INTRODUCTION

Scanning optical microscopy

Scanning optical microscopy is a powerful technique for imaging microstructures in biological systems at the cellular level. Cellular organelles stained with fluorescent dyes or auto-fluorescent structures inside cells can be imaged by raster-scanning a focused light source across the sample and collecting the fluorescence signal from each scanned position. In recent years, there have been various developments aimed at improving the spatial resolution of conventional microscopy; the most common is confocal microscopy. In this technique, a spatial filter is used in front of the photodetector to reject off-focal fluorescence, resulting in improved spatial resolution, especially in depth discrimination (Wilson, 1984, 1990). Another approach is two-photon fluorescence microscopy, in which a laser with high peak power is focused to a diffraction limited spot, inducing two-photon excitation of the chromophores. The quadratic dependence of excitation probability results in reduced fluorescence from off-focal axial planes, thus improving axial depth discrimination and localizing photobleaching to the focal volume (Denk et al., 1990). The optical sectioning effect in confocal and two-photon excitation microscopy allows three-dimensional imaging with superior resolution when compared to conventional fluorescence microscopy, although with less resolution than near-field microscopy (Betzig et al., 1993).

Lifetime-resolved fluorescence microscopy

In addition to intensity imaging with high spatial resolution, lifetime-resolved studies in fluorescence microscopy can provide additional insights into functionally important motions of biological systems. Dynamics of the chromophores in their local environments can be characterized, and such methods can help to elucidate functioning of cellular components at the molecular level. Many novel applications of fluorescence lifetime imaging have been demonstrated: important cellular information such as calcium concentration or cytoplasm matrix viscosity have been measured using lifetime-resolved methods (Dix and Verkman, 1990; Keating and Wensel, 1990; Kao et al., 1993). Measurement of the autofluorescence intensity and lifetime has been used to monitor the mechanism responsible for cell damage due to UVA exposure (Schneckenburger et al., 1992; Schneckenburger and Koenig, 1992; Koenig and Schneckenburger, 1994). Fluorescence lifetime has been used to assess antigen-processing stages in mouse macrophage cells (Voss, 1990). Furthermore, lifetime imaging can provide useful contrast between chromophores with similar emission spectra but different lifetimes (Draaijer et al., 1995). To improve the spatial resolution, lifetime-resolved methods can be implemented in a confocal (Morgan et al., 1991; Buurman et al., 1992) or two-photon (Piston et al., 1992) scanning microscope.

Lifetime-resolved imaging in the frequency domain requires the use of intensity modulated light sources (Gratton and Limkeman, 1983). For a species of chromophores with a single exponential lifetime τ and excited by sinusoidal excitation, $F(r, t)$, the density of fluorescence photons at position r and time t, obeys the differential equation

$$\frac{dF(r, t)}{dt} = -\frac{1}{\tau} F(r, t) + c\sigma q I(r, t), \qquad (1)$$

with sinusoidal excitation (photon flux) at modulation frequency ω and modulation m_e ($I(r, t) = [1 + m_e\sin(\omega t)]I(r)$).

The integrated fluorescence intensity is at the same circular frequency ω but is phase shifted and demodulated

$$F(t) = c\sigma q[1 + m_f\sin(\omega t + \phi)]\int I(r)\, d^3r, \qquad (2)$$

where c is the concentration of chromophores (assumed to be constant), σ is the absorption cross section, and q is the quantum yield. In solving Eqs. 1 and 2, one can obtain two independent determinations of the lifetime τ_p from phase shift ϕ, and τ_m from demodulation m (Lakowicz, 1983):

$$\tan(\phi) = \omega\tau_p \quad \text{and} \quad m = \frac{m_f}{m_e} = \frac{1}{\sqrt{1 + \omega^2\tau_m^2}}. \qquad (3)$$

More complex excitation modulation, such as a pulsed laser system, is the superposition of multiple sinusoidal Fourier components. In such a case, the fluorescence signal is the sum of the response to each Fourier component.

In studying ultrafast phenomena, fluorescence lifetime measurements are often limited by the detector time response. A typical photomultiplier (Hamamatsu R 928) used in a fluorescence lifetime instrument can be gain-modulated to about 300 MHz to study dynamic processes with a temporal resolution of 100 ps. A faster detector such as a microchannel plate has a frequency bandwidth up to about 10 GHz. On the other hand, a commonly available laser system can generate pulses with a width of about 1 ps corresponding to a frequency content up to 220 GHz (3 dB point). As a result, the standard frequency domain, fluorescence instrumentation is not capable of exploring the high-modulation frequency content offered by commonly available picosecond pulsed laser systems.

PUMP-PROBE FLUORESCENCE MICROSCOPY

Overview of pump-probe techniques

Pump-probe spectroscopy has been useful in elucidating fundamental processes in biology, chemistry, and condensed matter in the picosecond or sub-picosecond region. A common implementation of this technique is the transient absorption approach. One laser is beam-split and recombined spatially at the sample. Temporal evolution of the molecular dynamics is studied by varying the timing between the beam-split pulses by an optical delay line, and by recording the probe beam intensity at different delays, ultrafast temporal resolution can be achieved without high-speed detectors. In this methodology, a strong pump laser is used to excite the chromophores, and the weaker probe laser is used to monitor the return rate of the molecules to the ground state. A good signal-to-background ratio in the probe beam dictates that the pump beam be sufficiently strong to deplete the ground state population. This requirement results in strong absorption, and care has to be taken

to avoid photobleaching. There are different variations of the pump-probe techniques, but the central concept of using the optical delay line to study ultrafast dynamics remains the same (Evans, 1989; Fleming, 1986; Lytle et al., 1985). The ultimate temporal resolution of this type of pump-probe spectroscopy is determined by the pulsewidth of the laser, and at the present, the shortest pulsewidth achieved is less than 10 fs (Zhou et al., 1994). Ultrafast phenomena in many biological systems, including photosynthetic reaction centers, rhodopsin, and heme proteins, have been studied in this way (Hochstrasser and Johnson, 1988).

An alternative approach to using optical delay lines is the asynchronous sampling first proposed by the Lytle group (Elzinga et al., 1987). In this technique, a high repetition rate, pulsed laser (the pump) is focused to excite a fluorescent sample. A second pulsed laser (the probe) is focused onto the same spot to monitor the ground-state population or to induce stimulated emission from the sample. The pulsed repetition rates of the two lasers are slightly offset from each other, introducing a variable delay between the pump and probe. The effect of this delay is to repeatedly sample (probe) the population of the molecular excited state at multiple times after the pump beam excitation. In frequency space, the probe beam has a low-frequency component, at the difference of laser repetition (cross-correlation) frequencies. Because pulsed laser systems have harmonic content, cross-correlation signals between higher laser harmonics are also present in the probe beam, and these cross-correlation signals can be analyzed to obtain lifetime information of the sample.

To reduce photobleaching, an alternative method in pump-probe spectroscopy using stimulated emission can be used. In this case, the wavelength of the probe laser is chosen to induce stimulated emission from the excited state chromophores and instead of measuring the probe beam, the change in fluorescence is monitored. In this manner, photobleaching is reduced because it is not necessary to saturate the ground state, as is done in transient absorption studies. The stimulated emission approach has been recently demonstrated in spectroscopic studies (Lakowicz et al., 1994; Kusba et al., 1994).

Applications to microscopic imaging

In developing a pump-probe fluorometer in our laboratory, we realized that a new type of lifetime-resolved microscopy can be developed by applying the asynchronous sampling, stimulated emission approach inside a fluorescence microscope. Because only the molecules that interact with both the pump and probe lasers contribute to the cross-correlation signal, the strength of the signal depends critically on how well the two lasers are spatially overlapped. This introduces an axial sectioning effect similar to that of confocal and two-photon excitation microscopy. We can therefore expect greatly improved spatial resolution compared to conventional fluorescence microscopy. In addition, this in-

strument has the ultrafast time resolution characteristic of pump-probe methods without the need for fast optical detectors. The basic principle of our technique is illustrated in Fig. 1. Two pulsed lasers with slightly different repetition frequencies are overlapped at the sample. The lasers' wavelengths are chosen such that the pump beam is used to excite the chromophores under study and the probe beam is used to induce stimulated emission from the excited state molecules. With optical filtering, the fluorescence signal containing the cross-correlation harmonics can then be detected.

To see the unique features of this technique, consider a species of molecules that decays exponentially under sinusoidal excitation as described by Eqs. 1–3. Because stimulated emission propagates in the same direction as the radiation inducing such transition (Sargent et al., 1974), the sinusoidally modulated probe beam with intensity profile $I'(\vec{r}, t) = I'(\vec{r})I'(t) = I'(\vec{r})(1 + m'_e\sin(\omega' t + \phi'))$ causes a decrease in fluorescence collected by the same objective used in focusing and overlapping the two lasers. The observed fluorescence

$$F_{obs}(t) \alpha F(t) - \Delta F(t) \qquad (4)$$

changes by an amount proportional to the overlapping integral of the pump and probe beam profiles

$$\Delta F(t) \alpha c\sigma\sigma' q(1 + m'_e\sin(\omega' t + \phi'))(1 + m_f\sin(\omega t + \phi))$$

$$\cdot \int I(\vec{r})I'(\vec{r})\, d^3r, \qquad (5)$$

where σ' is the stimulated emission cross section. The product term $I(t)I(t')$ in Eq. (5) may be rewritten as the combination of two terms containing the sum and difference of frequencies ω and ω'. As a result, the measured fluorescence contains a cross-correlation term at the difference of the pump and probe beam repetition frequencies $|\omega' - \omega|$,

$$\Delta F_{cc}(t) \alpha c\sigma\sigma' q m_f m'_e\cos[|\omega' - \omega|t + (\phi' - \phi)]$$

$$\cdot \int I(\vec{r})I'(\vec{r})\, d^3r. \qquad (6)$$

In other words, with electronic filtering, the phase and modulation of the cross-correlation signal can be measured to determine the sample's lifetime using Eq. (3).

Superior spatial resolution provided by pump-probe fluorescence microscopy

A key feature in pump-probe fluorescence microscopy is the rejection of off-focal fluorescence, which results in improved spatial resolution compared to conventional microscopy. Fluorescence background is rejected because the pump-probe signal is localized near the focal region where both the pump and probe lasers have high photon flux. As Eq. 6 shows, in a pump-probe fluorescence microscope
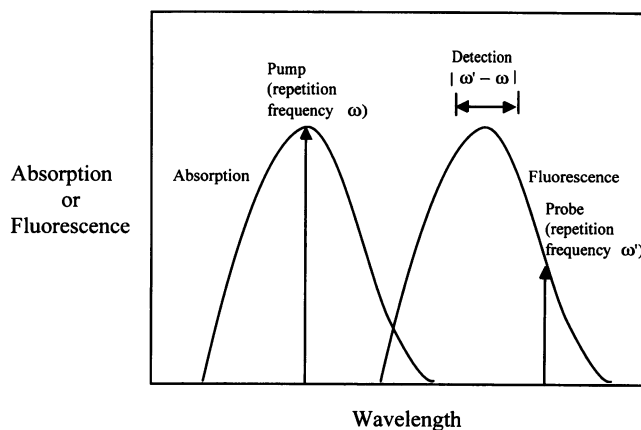

FIGURE 1 Principles of pump-probe (stimulated emission) techniques.

in which both the pump and probe processes involve a one-photon transition, the point spread function (PSF) is given by

$$I(u, v)I'(u', v') \qquad (7)$$

where

$$I(u, v) = \left| 2 \int_0^1 J_0(v\rho)e^{-(1/2)iu\rho^2} \rho\, d\rho \right|^2 \qquad (8)$$

is the PSF for conventional microscopy, $u = 2\pi(NA)^2 z/\lambda$ and $v = 2\pi(NA)r/\lambda$ are the respective optical coordinates in the axial and radial dimension, and λ is the wavelength of light focused by a circular objective with numerical aperture NA (Born and Wolf, 1985; Sheppard and Gu, 1990). Eq. (7) shows that the PSF $I(u, v)I'(u'v')$ is mathematically similar to the PSF of two-photon excitation microscopy $I(u/2, v/2)^2$, but at roughly half the wavelength. As a result, pump-probe fluorescence microscopy can provide better spatial resolution than two-photon excitation microscopy. Furthermore, the pump-probe PSF is identical to the PSF for confocal microscopy if the stimulated emission wavelength and the confocal detection wavelength are identical. Therefore, we expect comparable spatial resolution between pump-probe fluorescence microscopy and confocal microscopy.

Ultrafast molecular dynamics inside cells

Another unique feature of pump-probe fluorescence microscopy is lifetime-resolved imaging without the use of fast photodetectors. In Eqs. 4–6, we showed that the phase and amplitude of the cross-correlation signal at $|\omega' - \omega|$ can be used to determine the imaged sample's lifetime. In our experiments, $|\omega' - \omega|$ is chosen in the KHz range even though ω and ω' both can be in the 100 MHz range. In fact, for pulsed laser systems with harmonic content in the GHz range (220 GHz for a 1-ps laser), the frequency difference between specific harmonics can still be chosen to be in the

kilohertz range, to avoid the need for fast photodetectors. The frequency limit in studying ultrafast molecular phenomena is then determined by the harmonic contents of the light sources and the sample's frequency response rather than the speed of the photodetector.

In our study, we determined the signal saturation effect along with the spatial and temporal characteristics. The applications of this microscope to lifetime-resolved imaging are demonstrated in the following examples: lifetime-resolved imaging of fluorescent latex spheres, comparison of the pump-probe fluorescent image to one-photon image of labeled human erythrocytes and a mouse fibroblast cell, and imaging of a mouse fibroblast cell stained with multiple fluorescent probes.

METHODS

The experimental arrangement for our pump-probe fluorescence microscope is shown in Fig. 2.

Pump-probe light sources

A master synthesizer that generates a 10-MHz reference signal is used to synchronize two mode-locked neodymium-YAG (Nd-YAG, Antares, Coherent Inc., Santa Clara, CA) lasers and to generate a clock for the digitizer and scanner. The 532-nm output of the one Nd-YAG laser is used for excitation. The probe Nd-YAG laser pumps a DCM dye laser (Model 700; Coherent Inc.) tuned to 640 nm is used to induce stimulated emission. The pulsewidth (FWHM) of the pump laser is 150 ps, and the DCM probe laser has a pulsewidth of 10 ps. Combinations of polarizers are used to control the laser power reaching the sample. The average power of the pump and probe beams, at the sample, are about 10 μW and 7 mW, respectively. For time-resolved fluorescence microscopy, the pump source is operated at 76.2 MHz to 2.5 KHz and the probe laser's repetition frequency is 5 KHz away at 76.2 MHz + 2.5 KHz.

Scanning optics

The two lasers are combined at a dichroic mirror (Chroma Technology Inc., Brattleboro, VT) before reaching the x-y scanner (Cambridge Technology, Watertown, MA). The scanning mirrors can be driven by both analog and digital signal. We used the digital scheme to perform raster scans. The x and y scanners have a scanning range of ±60 degrees; each angular position is specified by a 16-bit binary number, but only the middle eight bits are used for scanning. This results in images composed of 256 ×

256 pixels. After the scanner, the laser beams enter the microscope system (Zeiss Axiovert 35, Thornwood, NY).

The epi-illuminated light path of the microscope has been modified to include a scan lens (10× eyepiece). It is positioned such that the x-y scanner is at its eye-point while the field aperture plane is at its focal point. The scan lens linearly transforms the angular deviation of the input laser beam controlled by the x-y scanner to a lateral translation of the focal point position at the field aperture plane. Because the field aperture plane is telecentric to the object plane of the microscope objective, the movement of the focal point on the object plane is proportional to the angular deviation of the scanned beam (Stelzer, 1995). The beams are then re-collimated by a tube lens before being reflected into the microscope objective by a second dichroic. To align the pump and probe lasers, we found it convenient to overlap their projections on the laboratory's ceiling.

For z-sectioning studies, it was necessary to vary the relative distance between the objective and the sample. Axial displacement of the objective is controlled by a stepping motor coupled to the objective manual adjustment mechanism and monitored by a linear variable differential transformer (LVDT; Schaevitz Engineering, Camden, NJ). This control system is designed to have a position resolution of 0.2 μm over a total axial range of 200 μm.

Because tight focusing increases the photon density and localizes the pump-probe effect, a high numerical aperture objective is used. The objective used in these studies is a well-corrected, Zeiss 63× Plan-Neofluar with numerical aperture (NA) of 1.25. The fluorescence signal is collected by the same objective and transmitted through the dichroic mirror and two 600 ± 20 nm bandpass filters before it is refocused onto the detector (R928 or R1104 photomultiplier tube; Hamamatsu, Bridgewater, NJ).

For normal operation, the pixel spacing in the images was 0.14 μm. A smaller stepping size of 0.035 μm was used when 0.28 μm fluorescent latex spheres are scanned to characterize the point spread function. The smaller step size was achieved by lowering two bits of the scanner driver.

Signal detection and processing

The analog PMT signal is electronically filtered by a pre-amplifier (Stanford Research, Sunnyvale, CA) to isolate the 5-KHz, cross-correlation signal. The filtered signal is then digitized by a 100-KHz, 12-bit sampling digitizer (A2D-160; DRA Laboratories, Sterling, VA). The Shannon Sampling Theorem dictates that at least two points per waveform must be acquired to determine a sinusoidal signal. We typically digitize four points per waveform to reduce harmonic noise. With four waveforms integrated per pixel, a pixel dwell time of 800 μs and a corresponding frame acquisition time of 52 s results. After digital processing, the amplitude and phase of the cross-correlation signal are then displayed and stored by the data acquisition computer.

Ultrafast spectroscopy demonstration

To demonstrate the potential of pump-probe fluorescence microscopy in obtaining high-frequency, lifetime-resolved information without fast optical detectors, a sample of rhodamine B in water was used. In this case, the pump laser is operated at 76.2 MHz and the probe laser's repetition frequency is at 76.2 MHz + 210 Hz. To enhance the signal-to-noise ratio at higher cross-correlation harmonics, we found that it was necessary to increase the pump laser power to 35.6 μW (the probe laser power set to 2.75 mW). The fluorescence signal was collected and optically filtered in the same manner as for imaging, and the photomultiplier signal is fed directly into a spectrum analyzer (Hewlett Packard 35665A, Rolling Meadows, IL), where the harmonics are displayed and stored at the bandwidth of 16 Hz.
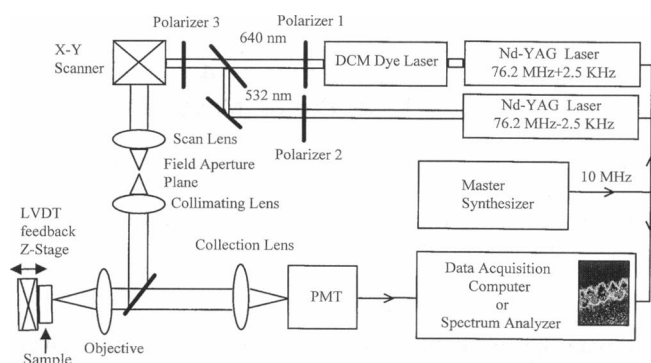

FIGURE 2   Pump-probe (stimulated emission) fluorescence microscope.

RESULTS AND DISCUSSION

Pump-probe signal dependence on laser power level

We have investigated the dependence of the cross-correlation signal on the pump and probe laser powers. As the pump or probe laser power is increased, eventually the signal will saturate because of the depletion of chromophores in the focal volume available for the pump-probe process. Off-focal signal can begin to contribute significantly, resulting in broadening of the point spread function and deterioration of the spatial resolution.

For the saturation test, aqueous rhodamine B (4.16 mM) sealed (with nail polish) between the coverslip and a microscope slide was used. The test was performed in two steps. First, the fluorescence saturation effect due to the pump source is determined by focusing different intensity of the excitation laser onto the rhodamine B sample and recording the PMT output induced by the fluorescence. The result is shown in Fig. 3 a, where the effect of saturation is evident starting at about 10 μW. Next, the probe laser was also focused onto the rhodamine B sample, and the first harmonic amplitude at 5 KHz was recorded at three different pump laser settings of 1.75, 3.18, and 5.12 μW; all are in the linear region of the fluorescence curve shown in Fig. 3 a. The three calibration curves are plotted in Fig. 3 b along with best linear fits using first five points of each data set. The slopes of the three calibration curves are plotted as a function of pump power in Fig. 3 c. Fig. 3 b shows that the pump-probe signal deviates from linearity starting at about 7 mW of the probe laser at 640 nm. The linearity in the slope plot of Fig. 3 c confirms that the cross-correlation signal is proportional to the intensity of both the pump and probe sources if the power levels used do not exceed 10 μW (pump) and 7 mW (probe). These values also represent the upper limits in power levels used in our experiments. Note that the beginning power for the probe laser saturation is more than two orders of magnitude higher than that for the pump laser. The difference in power may be due to several factors. First, the absorption and stimulated emission cross sections may be quite different at the wavelengths chosen. For rhodamine 6G, a related species of rhodamine B, the absorption (at 532 nm) and stimulated emissions (at 640 nm) are about 2.6×10^{-16} cm^2 and 4.0×10^{-17} cm^2, respectively (Penzkofer and Leupacher, 1987). The difference in cross sections can contribute to an order of magnitude higher probe laser power needed in observing saturation effects. Other factors such as pump and probe beam overlapping efficiency, excited state molecule rotational effects, and quantum efficiency can also contribute to the higher probe laser power needed to observe saturation effects in the cross-correlation signal.

The linearity calibration data are valid only for rhodamine B in water at the wavelengths chosen. The estimation of the power for pump saturation may be extended to other chromophores if their extinction coefficients are known. To
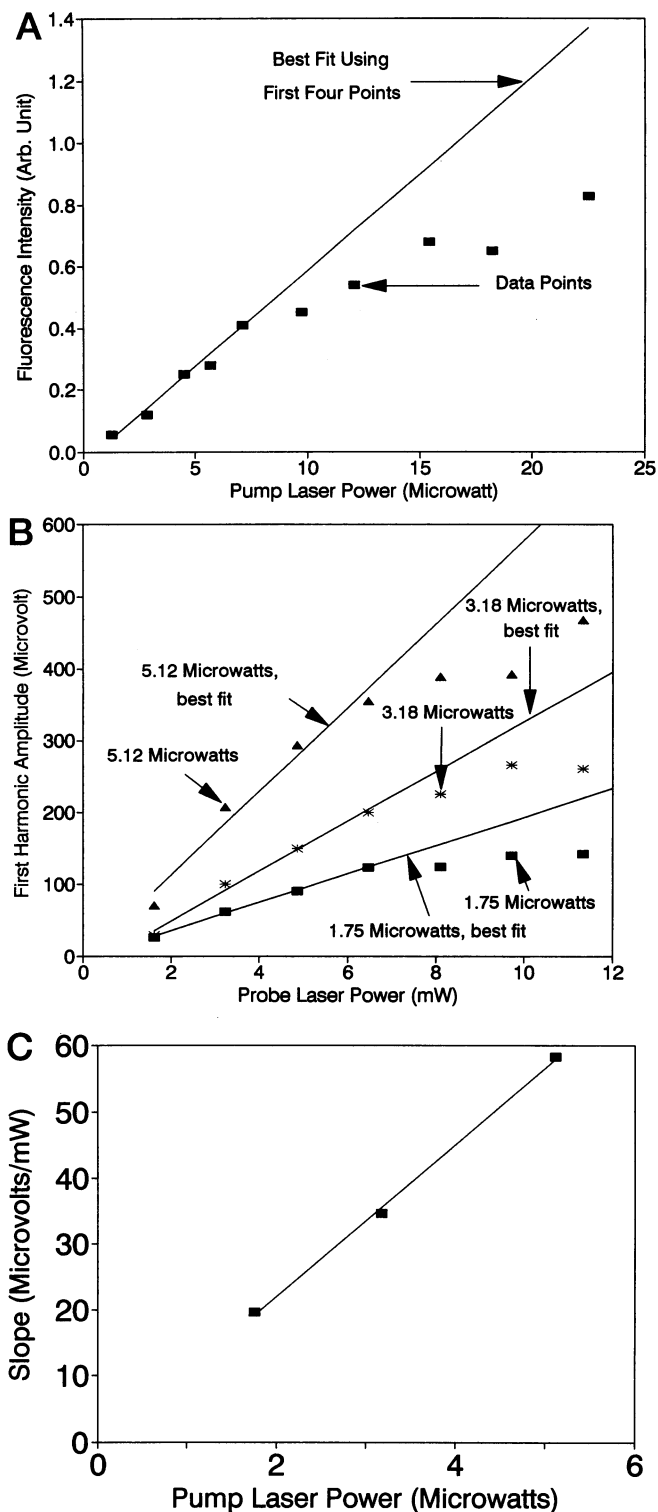

FIGURE 3   (a) Fluorescence generated as a function of pump beam intensity (532 nm). (b) First harmonic amplitude at different pump and probe (640 nm) intensities. (c) Slope of first harmonic amplitude plots at different pump powers.

estimate the probe beam saturation power for other chromophores, their cross sections relative to that of rhodamine B in water need to be determined. Because rhodamine B has

relatively strong absorption compared to many other dyes, to avoid PSF broadening in imaging experiments where the chromophores' spectroscopic properties are not always known, the power levels chosen were around 10 μW for the pump beam and 7 mW for the probe beam, both in the linear region for rhodamine B's pump-probe signal.

Spatial resolution in pump-probe fluorescence microscopy

To characterize the radial and axial spatial resolution of the system, orange fluorescent latex spheres of 0.28 μm diameter (absorption maximum: 530 nm, emission maximum: 560 nm; Molecular Probes, Eugene, OR) were imaged. These spheres were immobilized between a coverslip and a flat microscope slide with Fluoromount G mounting medium (Southern Biotechnology, Birmingham, AL). The slide was left to dry at room temperature for 1 day before the spheres were imaged. The size of the spheres was uniform and calibrated by the manufacturer using electron microscopy. Because the dimensions of the spheres are comparable to the FWHM of the theoretical pump-probe PSF at the wavelengths chosen, the fluorescence intensity measured is compared with the convolution of the theoretical PSF to the sphere size given by

$$I_{\text{sphere}}(z, r) = \frac{I(z, r)I'(z, r) \otimes S(z, r)}{I(0, 0)I'(0, 0) \otimes S(0, 0)}, \tag{9}$$

where $S(z, r)$ characterizes the physical dimension of the spheres in the axial (z) and radial (r) dimension; it has the value of 1 for $\sqrt{z^2 + r^2} \leq 0.14$ μm, 0 otherwise. Data from 36 spheres were analyzed, and the experimental and theoretical intensity distributions are plotted in Fig. 4. Although the axial data agree well with the Fraunhofer diffraction theory, there is deviation of the radial data from the theoretical prediction. This deviation is probably due to slight misalignment of the pump and probe lasers. Other possible effects include chromatic aberrations and the polarization effect of the focusing objective.

Potential for studying ultra-fast molecular dynamics

A slide of 4.16 mM rhodamine B in water was used to demonstrate the potential of pump-probe fluorescence microscopy in providing lifetime-resolved, high-frequency images without a fast optical detector. By using a spectrum analyzer, rhodamine B's power spectrum was recorded up to about 6.7 GHz (Fig. 5). Higher frequency harmonics may be measured if the frequency bandwidth is decreased further (Berland et al., 1992). Note that the harmonics displayed begins at 210 Hz, the first harmonic, and are separated by the same frequency difference of 210 Hz. However, because of the frequency translation effect of beams beating, the harmonics actually correspond to the sample's response at harmonics of the fundamental excitation frequency of 76.2
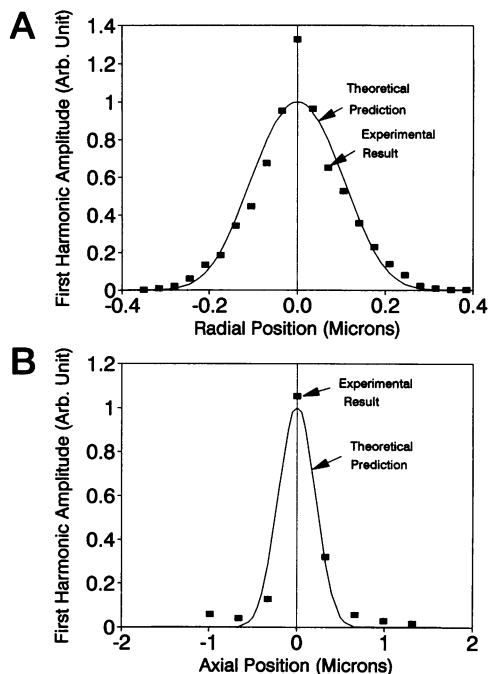

FIGURE 4   (a) Radial intensity response, and (b) axial intensity response of 0.28 μm orange fluorescent latex spheres.

MHz. The decay in amplitude as the frequency increases corresponds to the decrease in modulation predicted in Eq. 6. By fitting the decay using the first twelve harmonics, the lifetime of rhodamine B in water is determined to be 1.44 ns, in good agreement with the 1.5 ns measured by standard frequency-domain phase fluorometry. Due to the signal-to-noise considerations, higher order harmonics are not used in the fit. The measured lifetime of 1.44 ns is used as the reference lifetime in analyzing lifetime-resolved images in the next section. Fig. 5 demonstrates the potential of obtaining high-frequency images of biological systems by measuring the cross-correlation signal at low frequencies.
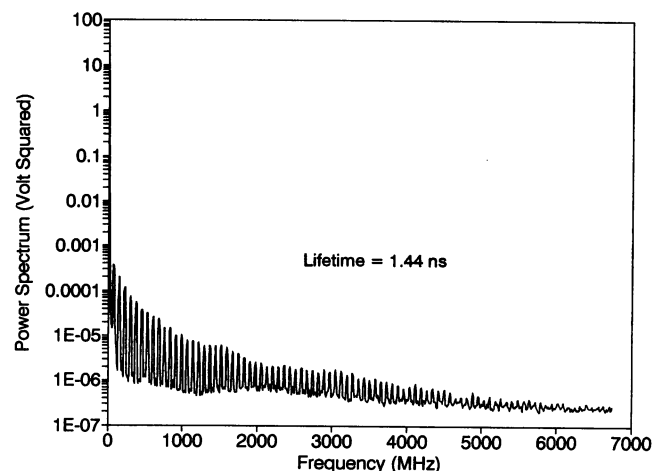

FIGURE 5   High-frequency spectra of 7.8 mM rhodamine B in water ($\tau_m = 1.44$ ns).

Any harmonic displayed in the figure can be used for imaging purposes. The ultimate limit in imaging with a higher order harmonic is due to the signal-to-noise consideration. Although we have shown the high-frequency response in the GHz region, there is no particular difficulty in performing the experiments in the lower frequency region. Because multiple harmonics are present in the fluorescence signal, the next step in our study is to implement parallel acquisition to measure them simultaneously using a high-speed digitizer. The phase shift and amplitude of each cross-correlation harmonic can then be measured to determine the chromophores' lifetimes at different excitation modulation frequencies.

Applications to lifetime-resolved imaging

Imaging of fluorescent latex spheres

We obtained lifetime-resolved images of a mixture of 2.3-μm orange and 1.09-μm Nile-red (absorption maximum: 520 nm; emission maximum: 580 nm) fluorescent latex spheres (Molecular Probes, Eugene, OR). The two types of spheres were known to have different lifetimes. The measured lifetimes using standard frequency domain phase fluorometry are 2.70 ns for 1.09-μm spheres and 4.28 ns for 2.3-μm spheres. In our images, the first harmonic amplitude and phase are measured (Fig. 6). The phase image was referenced to that of a 4.16 mM rhodamine B slide for the purpose of lifetime calculations. From the histograms of lifetime values, the lifetimes of the spheres were determined to be 3.2 ± 1.0 ns (1.09 μm) and 4.2 ± 1.4 ns (2.3 μm). These values agree within error with the results from frequency domain phase fluorometry.
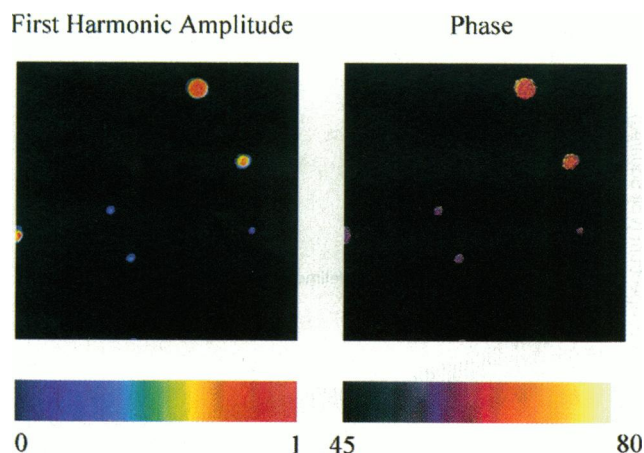
Comparison between conventional microscopy and pump-probe fluorescence microscopy in human erythrocytes and mouse fibroblast

To demonstrate the superior spatial resolution achieved by pump-probe fluorescence microscopy compared to conventional one-photon microscopy, we imaged two commonly used biological systems: human erythrocytes and mouse fibroblast cells.

The human erythrocytes were labeled with the membrane dye rhodamine DHPE (Molecular Probes). A small amount of erythrocytes was mixed with Hanks' balanced salt buffer (HBSB with NaHCO$_3$) to make a 1-ml mixture. The solution was spun at 1000 rpm for 5 min before the top buffer was removed. The erythrocytes were then shaken and diluted to 1 ml with HBSB. Six microliters of rhodamine DHPE (at 5 mg/ml dimethylsulfoxide) was injected into the solution containing the cells and allowed to incubate for 30 min. After incubation, the cells were again spun down and washed with HBSB two more times to remove residual dye before mounting onto a microscope slide. Nail polish was used to seal the coverslip.

The mouse fibroblast cells were grown on a coverslip. For fixation, they were placed in acetone for 5 min and allowed to air dry. Then, a few drops of a solution containing 10 μg/ml of rhodamine DHPE (diluted in phosphate-buffered saline (PBS), 0.1% Triton X-100) were placed onto the coverslip and incubated for 30 min. After incubation, the dye was removed by rinsing the coverslip in PBS buffer twice before mounting on a flat microscope slide. For mounting, a drop of the mounting medium Prolong (Molecular Probes) was placed between the coverslip and a slide. In a few hours the mounting medium had dried and the slide was ready for viewing.

The images at the first harmonic of 5 KHz are presented in Fig. 7, along with the corresponding one-photon images. The one-photon images were obtained by blocking the probe beam and recording only the fluorescence intensity due to the pump beam. In this manner, the cells were not moved relative to the microscope objective and a comparison between the two techniques can be made. From the erythrocytes' image, it is apparent that the pump-probe images can better reject the fluorescence from off-focal planes. The one-photon images show much more background fluorescence from the central region of the erythrocytes than pump-probe microscopy. Similarly, the pump-probe image of the mouse fibroblast shows superior spatial resolution compared to the corresponding one-photon image by revealing the finer details of the cell's structure.

Multiple dye labeled mouse fibroblast

We examined mouse fibroblast cells doubly labeled with the nucleic acid stain ethidium bromide and the membrane stain rhodamine DHPE (Molecular Probes). The pump-probe image is shown in Fig. 8. These cells (grown on a coverslip) are fixed and stained in the same manner as the mouse
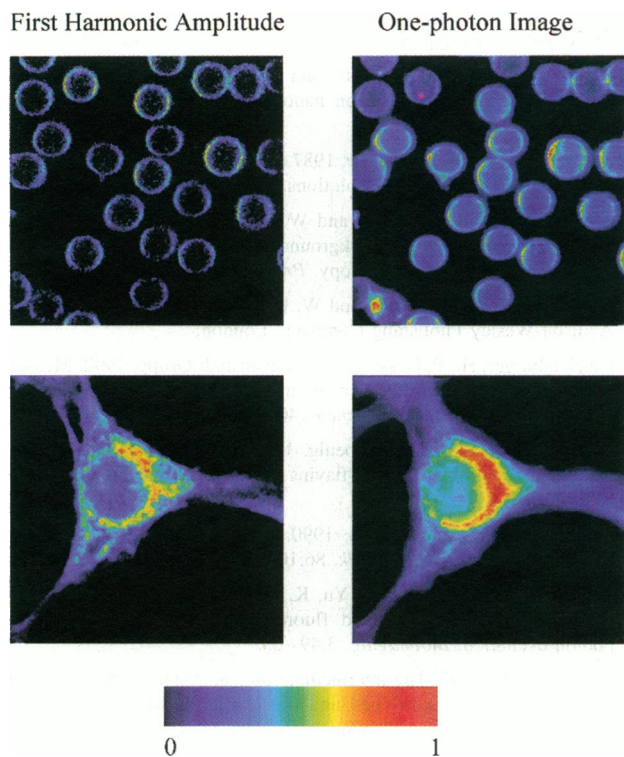

First Harmonic Amplitude   Phase

0   1   45   80

FIGURE 6   Time-resolved images of 1.09 μm Nile red (τ_p = 3.2 ± 1.0 ns) and 2.3 μm orange (τ_p = 4.2 ± 1.4 ns) fluorescent latex spheres, first harmonic amplitude normalized. Phase is in degrees.

FIGURE 7　Comparison of pump-probe fluorescence and one-photon excitation images, first harmonic amplitude normalized. (*Top*) Human erythrocytes; (*bottom*) a mouse fibroblast cell. Staining: rhodamine DHPE.

fibroblast cell discussed above. The only difference is that the coverslip was covered first with ethidium bromide (1 mM in PBS, 0.1% Triton X-100) for 30 min and then stained by rhodamine DHPE (10 μg/ml in PBS, 0.1% Triton X-100) for another 30 min before it was rinsed twice in PBS and mounted for viewing. The lifetimes of the cytoplasmic and nuclear region were determined from the phase image.
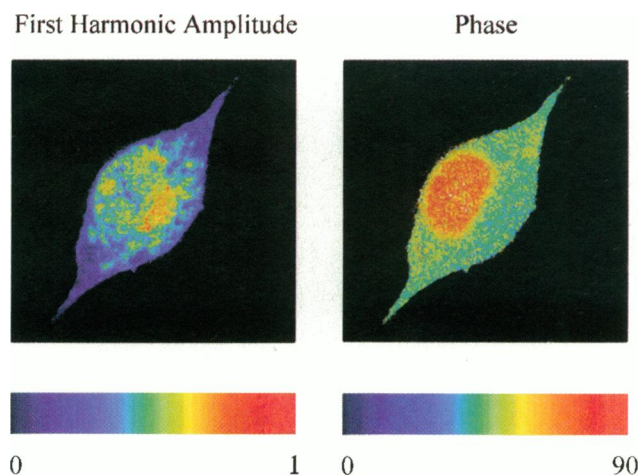

FIGURE 8　Time-resolved images of a mouse fibroblast cell labeled with rhodamine DHPE and ethidium bromide (membrane and cytoplasm: τ_p = 2.0 ± 0.5 ns; nucleus: τ_p = 6.6 ± 4.8 ns), first harmonic amplitude normalized. Phase is in degrees.

The reference phase was obtained from a slide of 4.16 mM rhodamine B in water. It was found that the average of lifetime histograms in the cytoplasm and nucleus are 2.0 ± 0.5 ns and 6.6 ± 4.8 ns, respectively. For comparison, the lifetime of rhodamine B in water was determined from standard frequency domain phase fluorometry to be 1.5 ns. Furthermore, the lifetimes of the unbound ethidium bromide and ethidium bromide bound to nucleic acid are known to be 1.7 and 24 ns, respectively (So et al., 1995). Our measurements of lifetime in cytoplasm show that there was significant staining of cytoplasmic structures by rhodamine DHPE. The average lifetime in the nucleus is between that of bound and unbound ethidium bromide, indicative of the fact that both populations of the chromophores exist in the nucleus. Nonetheless, the lifetime contribution from bound ethidium bromide is sufficient to distinguish the different lifetimes in the nucleus and cytoplasm as demonstrated by the phase image.

This example demonstrates one advantage of lifetime-resolved imaging. From intensity imaging, it is difficult to distinguish the cytoplasmic and nuclear regions, because these chromophores have similar emission spectra. With lifetime imaging, a sharp contrast between the different species of chromophores can be generated.

CONCLUSION

We have demonstrated the first application of the asynchronous, pump-probe, stimulated emission technique to fluorescence microscopy. By measuring the fluorescence signal at the cross-correlation frequency, pump-probe fluorescence microscopy can provide superior spatial resolution and effective off-focal background rejection compared to conventional one-photon microscopy. Because of the wavelengths used in the one-photon pumping and probing processes, this technique has better spatial resolution than two-photon excitation microscopy, and comparable spatial resolution as confocal microscopy. Furthermore, imaging at low-frequency, cross-correlation harmonics eliminates the need of using a fast optical detector in lifetime-resolved imaging of biological systems.

REFERENCES

Berland, K. M., E. Gratton, and M. J. vandeVen. 1992. A laser heterodyning detector for frequency domain ultrafast spectroscopy. Time-resolved laser spectroscopy in biochemistry III. *SPIE Proc.* 1640:370–378.

Betzig, E., R. J. Chichester, F. Lanni, and D. L. Taylor. 1993. Near-field fluorescence imaging of cytoskeletal actin. *Bioimaging.* 1:129–135.

Born, M., and E. Wolf. 1985. Principles of Optics, 5th ed. Pergamon Press, Oxford.

Buurman, E. P., R. Sanders, A. Draaijer, H. C. Gerritsen, J. J. F. Van Veen, P. M. Houpt, and Y. K. Levine. 1992. Fluorescence lifetime imaging using a confocal laser scanning microscope. *Scanning.* 14:155–159.

Denk, W., J. H. Strickler, and W. W. Webb. 1990. Two-photon laser scanning fluorescence microscopy. *Science.* 248:73–76.

Dix, J. A., and A. S. Verkman. 1990. Pyrene excimer mapping in cultured fibroblasts by ratio imaging and time-resolved microscopy. *Biochemistry.* 29:1949–1953.

Draaijer, A., R. Sanders, and H. C. Gerritsen. 1995. Fluorescence lifetime imaging, a new tool in confocal microscopy. *In* Handbook of biological Confocal Microscopy, J. Pawley, editor. Plenum Press, New York.

Elzinga, P. A., R. J. Kneisler, F. E. Lytle, G. B. King, and N. M. Laurendeau. 1987. Pump/probe method for fast analysis of visible spectral signatures utilizing asynchronous optical sampling. *Appl. Optics.* 26:4303–4309.

Elzinga, P. A., F. E. Lytle, Y. Jian, G. B. King, and N. M. Laurendeau. 1987. Pump/probe spectroscopy by asynchronous optical sampling. *Appl. Spectrosc.* 41:2–4.

Evans, D. K. editor. 1989. Laser Applications in Physical Chemistry. Marcel Dekker, New York.

Fleming, G. R. 1986. Chemical Applications of Ultrafast Spectroscopy. Oxford University Press, New York.

Gratton, E., and M. Limkeman. 1983. A continuously variable frequency cross-correlation phase fluorometer with picosecond resolution. *Biophys. J.* 44:315–324.

Hochstrasser, R. M., and C. K. Johnson. 1988. Biological processes studied by ultrafast laser techniques. *In* Ultrashort Laser Pulses, W. Kaiser, editor. Springer-Verlag, New York. 357–417.

Kao, H. P., J. R. Abney, and A. S. Verkman. 1993. Determinants of the translational mobility of a small solute in cell cytoplasm. *J. Cell Biol.* 120:175–184.

Keating, S. M., and T. G. Wensel. 1990. Nanosecond fluorescence microscopy: emission kinetics of fura-2 in single cells. *Biophys. J.* 59:186–202.

Koenig, K., and H. Schneckenburger. 1994. Laser-induced autofluorescence for medical diagnosis. *J. Fluorescence.* 4:17–40.

Kusba, J., V. Bogdanov, I. Gryczynski, and J. R. Lakowicz. 1994. Theory of light quenching: effects on fluorescence polarization, intensity, and anisotropy decays. *Biophys. J.* 67:2024–2040.

Lakowicz, J. R. 1983. Principles of Fluorescence Spectroscopy. Plenum Press, New York.

Lakowicz, J. R., I. Gryczynski, V. Bogdanov, and J. Kusba. 1994. Light quenching and fluorescence depolarization of rhodamine B. *J. Phys. Chem.* 98:334–342.

Lytle, F. E., R. M. Parrish, and W. T. Barnes. 1985. An introduction to time-resolved pump/probe spectroscopy. *Appl. Spectrosc.* 39:444–451.

Morgan, C. G., A. C. Mitchell, and J. G. Murray. 1991. Prospects for confocal imaging based on nanosecond fluorescence decay time. *J. Microsc.* 165:49–60.

Penzkofer, A., and W. Leupacher. 1987. Fluorescence behaviour of highly concentrated rhodamine 6G solutions. *J Luminescence.* 37:61–72.

Piston, D. W., D. R. Sandison, and W. W. Webb. 1992. Time-resolved fluorescence imaging and background rejection by two-photon excitation in laser scanning microscopy. *Proc. SPIE.* 1640:379–389.

Sargent, M., III, M. O. Scully, and W. E. Lamb, Jr. 1974. Laser Physics. Addison-Wesley Publishing Company, London.

Schneckenburger, H., P. Gessler, and I. Pavenstadt-Grupp. 1992. Measurement of mitochondrial deficiencies in living cells by microspectrofluorometry. *J. Histochem. Cytochem.* 40:1573–1578.

Schneckenburger, H., and K. Koenig. 1992. Fluorescence decay kinetics and imaging of NAD(P)H and flavins as metabolic indicators. *Opt. Eng.* 31:1447–1451.

Sheppard, C. J. R., and M. Gu. 1990. Image formation in two-photon fluorescence microscopy. *Optik.* 86:104–106.

So, P. T. C., T. French, W. M. Yu, K. M. Berland, C. Y. Dong, and E. Gratton. 1995. Time-resolved fluorescence microscopy using two-photon excitation. *Bioimaging.* 3:49–63.

Stelzer, E. H. K. 1995. The intermediate optical system of laser-scanning confocal microscopes. *In* The Handbook of Biological Confocal Microscopy. J. Pawley, editor. Plenum Press, New York. 139–153.

Voss, E. 1990. Anti-fluorescein antibodies as structure-function models to examine fundamental immunological and spectroscopic principles. *Commun. Mol. Cell Biophys.* 6:197–221.

Wilson, T., editor. 1990. Confocal Microscopy. London: Academic Press.

Wilson, T., and C. Sheppard. 1984. Theory and Practice of Scanning Optical Microscopy. Academic Press, London.

Zhou, J., G. Taft, C. P. Huang, I. P. Christov, H. C. Kapteyn, and M. M. Murnane. 1994. Sub-10 fs pulse generation in Ti:sapphire: capabilities and ultimate limits. *In* Ultrafast Phenomena IX, P. F. Barbara, W. H. Knox, G. A. Mourou, and A. H. Zewail, editors. Springer-Verlag, Berlin. 39–40.